Anomalous magnetic exchange interactions in $SmCu_2$

M. Rotter,* M. Doerr, M. Loewenhaupt, and U. Witte
Institut für Angewandte Physik, Technische Universität Dresden, D-01062 Dresden, Germany

P. Svoboda and J. Vejpravová
Department of Electronic Structures, Charles University, 12116 Prague 2, Czech Republic

H. Sassik
Institut für Experimentalphysik, Technische Universität Wien, Wiedner Hauptstraße 8-10, A-1040 Wien, Austria

C. Ritter
Institut Laue Langevin, F-38042 Grenoble, France

D. Eckert, A. Handstein, and D. Hinz
Institut für Festkörper- und Werkstofforschung, P.O.B. 270116, D-01171 Dresden, Germany
(Received 7 February 2001; revised manuscript received 21 June 2001; published 31 August 2001)

RCu_2 compounds (R = rare earth) show magnetic structures with very different propagation vectors. This behavior can be explained by the anisotropy of the magnetic exchange interaction in combination with the crystal field. In order to support this model the magnetic phase diagram of a $SmCu_2$ single crystal has been investigated by magnetization, thermal expansion, magnetostriction, electrical transport, and specific heat measurements. The magnetic structure in zero field has been determined by neutron diffraction on a powder sample using ^{154}Sm. The magnetic moments were found to be oriented parallel to the b direction in contrast to other RCu_2 compounds (R = Tb, Dy, Ho) with the same propagation. In order to explain the observed magnetic structure of $SmCu_2$ we infer that the anisotropic part of the exchange interaction tensor is reversed in comparison with the other RCu_2 compounds.

DOI: 10.1103/PhysRevB.64.134405 PACS number(s): 75.30.Et, 75.30.Gw, 75.50.−y

I. INTRODUCTION

There are two kinds of magnetic anisotropy in rare-earth compounds: the single-ion anisotropy caused by the crystal field (CF) and the anisotropy of the two ion interactions. Both types of anisotropy have to be considered to arrive at a consistent description of the magnetic properties of the orthorhombic intermetallic compound $NdCu_2$ (Refs. 1–3) (space group *Imma*).

The exchange parameters determined from inelastic neutron-scattering experiments on $NdCu_2$ (Ref. 1) can be used to make a prediction for the ordering temperature and the magnetic structure of some other isostructural RCu_2 compounds on the basis of a mean-field theory. These agree well with the available experimental results for the $TbCu_2$, $DyCu_2$, and $TmCu_2$ compounds[1]: the magnetic ordering vector $\boldsymbol{\tau}$ is determined by the magnetic exchange interaction and depends on the moment direction, because the exchange interaction is anisotropic. If the magnetic moments point into the crystallographic b direction due to the CF, an ordering wave vector of $\boldsymbol{\tau}\sim(2/3\ 0\ 0)$ is expected (as observed for $NdCu_2$ and $TmCu_2$). If the moments are oriented perpendicular to b then the ordering wave vector is $\boldsymbol{\tau}=(2/3\ 1\ 0)$ (e.g., for $TbCu_2$ and $DyCu_2$).

$SmCu_2$ is a compound of this series that has not been investigated by neutron scattering due to the high absorption cross section of Sm. The measurement of the susceptibility indicates that in this compound an antiferromagnetic ordering occurs below 23 K with a magnetic moment in b direction similar to the case of $NdCu_2$ and $TmCu_2$.[4,5] As in $NdCu_2$ the measurements of the specific heat gave evidence for a second transition at 17 K, which probably is connected with a change of the ordering vector from a commensurate to an incommensurate value. If the model mentioned above is correct we would expect to find an antiferromagnetic ordering with a wave vector of about $\boldsymbol{\tau}=(2/3\ 0\ 0)$.

II. EXPERIMENT

To clarify the magnetic ordering process in $SmCu_2$ we performed a neutron-diffraction experiment on a polycrystalline sample prepared with the isotope ^{154}Sm in order to reduce the absorption cross section. The polycrystalline sample for this neutron-scattering experiment was prepared at the Technical University (Vienna) by arc melting stoichiometric amounts of ^{154}Sm and Cu in protective argon atmosphere. Phase purity was checked by x-ray powder diffraction. The D1B diffractometer of the Institut Laue Langevin (Grenoble) was used because of its high resolution at low angles and its high flux of $6.5\times10^6\ n\,cm^{-2}\,s^{-1}$ at the sample position (which was essential for the small sample of 3 g with a small magnetic moment). To determine the temperature dependence of the magnetic structure a profile analysis at temperatures $T=2$, 20, and 30 K was performed using a wavelength of 0.25 nm. The data were fitted using the FULLPROF profile matching program. The diffraction pattern at 2 K was used to refine the structural parameters and the size of the magnetic moment at the same time. The refined unit-cell parameters at 2 K are $a=0.436\pm0.003$ nm, $b=0.685\pm0.006$ nm, $c=0.735\pm0.006$ nm; the atomic position parameters are

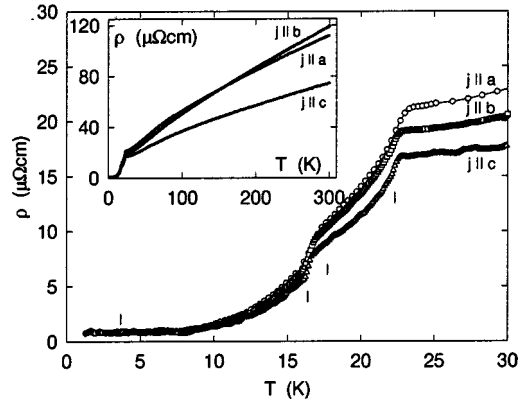

FIG. 1. Low-temperature part of the temperature dependence of the electrical resistivity parallel to the main crystallographic axes. The inset shows the resistivity up to the room temperature.

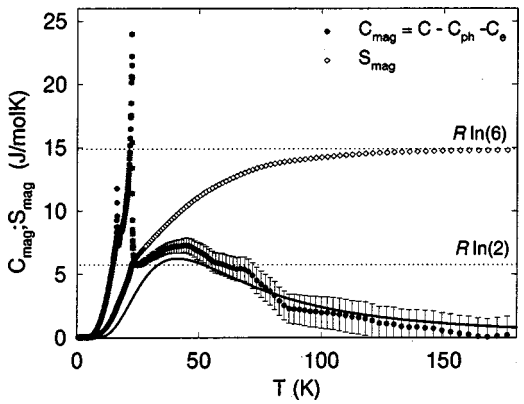

FIG. 2. Analysis of the magnetic part of specific heat together with the magnetic entropy. The full line shows the best fit of a Schottky contribution and the dashed lines correspond to the entropy of doublet and sextet, respectively.

$z_{\mathrm{Sm}}=0.544\pm0.004$, $y_{\mathrm{Cu}}=0.055\pm0.001$, and $z_{\mathrm{Cu}}=0.170\pm0.001$.

The magnetic and dilatometric measurements were performed on a single crystal with dimensions $2.2\times2.9\times2.1$ mm^3. The single crystal of $SmCu_2$ was grown by the Czochralski pulling method using the tri-arc furnace at Charles University (Prague). We have used about 10 g of melt, consisting of pure constituents of Sm (3N5) and Cu (5N). The melt was kept in water-cooled copper crucible under pure argon (6N) protective atmosphere (pressure 1.3 bar). Due to the high volatility of Sm, 5 at.% of Sm was added to the stoichiometric composition. The growing conditions were as follows. Pulling speed: 10 mm/hour, rotation of the seed: 20 min^{-1}, rotation of the crucible: 10 min^{-1}. We have succeeded in growing a single-crystalline ingot about 40 mm long with 4 mm maximum diameter. X- ray diffraction (using Cu-Kα_1-Kα_2 radiation) was done afterwards to check the phase purity and to measure the lattice parameters of the single crystal at room temperature. The lattice parameters were found to be $a=0.43577\pm0.00003$ nm, $b=0.69343\pm0.00005$ nm, $c=0.73720\pm0.00006$ nm and the atomic positions are $z_{\mathrm{Sm}}=0.545\pm0.001$, $y_{\mathrm{Cu}}=0.065\pm0.001$, and $z_{\mathrm{Cu}}=0.165\pm0.001$. All these parameters agree very well with those reported in the literature.[5] No other phase (even oxides) was observed within the precision of the x rays. Measurements of the temperature dependence of the electrical resistivity parallel to the main crystallographic axes (see Fig. 1) have also confirmed the high quality of the single crystal, yielding the residual resistivity ratios RRR=155, 175, and 78.5 for the current along *a*, *b*, and *c* axis, respectively (see the inset of Fig. 1).

Thermal expansion and magnetostriction was measured using a capacitance dilatometer in a 15 T Oxford Instruments superconducting magnet,[6] magnetization measurements were performed in a vibrating sample magnetometer (Oxford Instruments) in steady fields up to 14 T and in the 50 T pulsed field magnet of the Dresden high field facility.[7] Electrical resistivity and isobaric specific heat of $SmCu_2$ in the zero magnetic field were measured in the temperature range 0.5–300 K using a PPMS facility (Quantum Design).

III. RESULTS AND DISCUSSION

A. Specific heat

The results of specific heat measurements are shown in Figs. 2 and 3. For the analysis of the isobaric specific heat c_p we have considered three main contributions:

$$c_p=c_e+c_{ph}+c_{mag}, \tag{1}$$

where c_e is the electronic part, expressed as $c_e=\gamma T$ (γ denotes the Sommerfeld constant), c_{ph} is the phonon part, including the anharmonic effect,[8] written in the form

$$c_{ph}=\frac{9R_g}{1-\alpha_D T}\left(\frac{1}{x_D}\right)^3\int_0^{x_D}\frac{x^4\exp(x)}{[\exp(x)-1]^2}dx, \tag{2}$$

where $x_D=\Theta_D/T$, Θ_D is the Debye temperature, α_D is the anharmonic correction term, and R_g is the gas constant.

The magnetic part of the specific heat is caused by the magnetic exchange field (below T_N, for a discussion of the magnetic phases we refer to the Sec. III B) in addition to the crystal field. The orthorhombic crystal field splits the $4f^5$ ground state of the Sm^{3+} ion ($J=5/2$, $L=5$, $S=5/2$) into 3

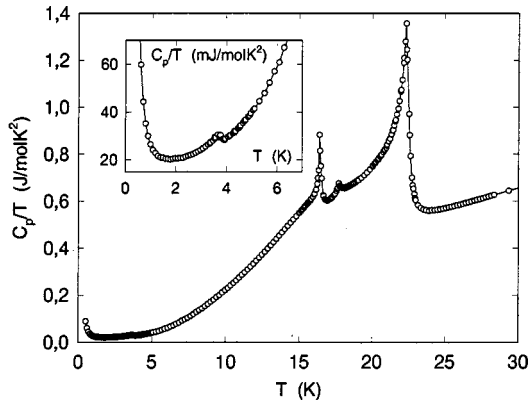

FIG. 3. Low-temperature part of the specific heat of $SmCu_2$ in the C/T vs T representation indicating the magnetic phase transitions at $T=16.4$, 17.7, and 22.3 K, respectively. The inset shows the anomaly corresponding to the lowest phase transition at 3.7 K.

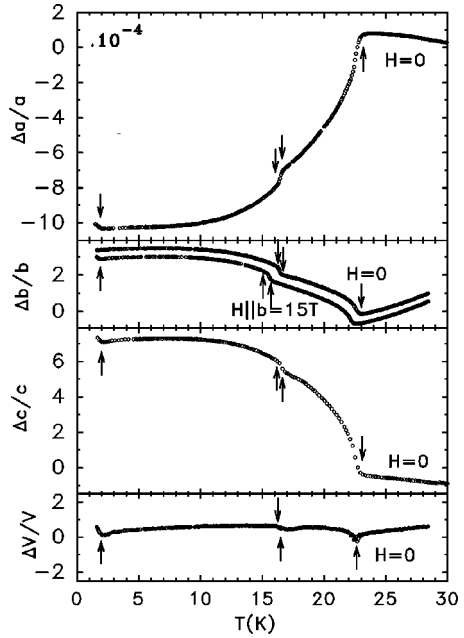

FIG. 4. Thermal expansion of $SmCu_2$ along the crystallographic a,b, and c directions at zero magnetic field. The relative volume change as deduced from $\Delta V/V=\Delta a/a+\Delta b/b+\Delta c/c$ is shown at the bottom. For the b direction also the 15 T curve is shown.

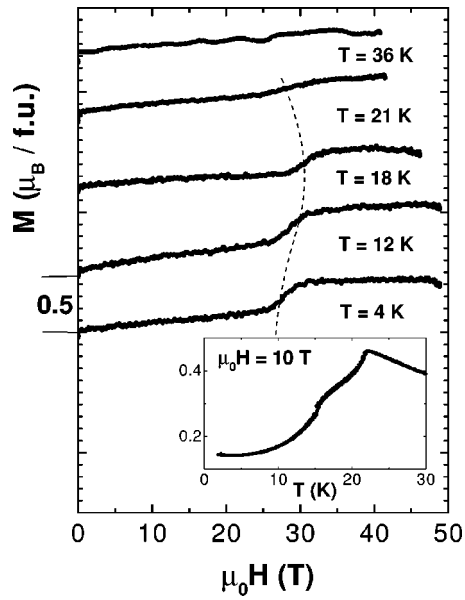

FIG. 5. Magnetization of $SmCu_2$ along the crystallographic b direction measured at different temperatures in a pulsed magnetic field. The inset shows the temperature dependence of the magnetization measured along b in a steady field of 10 T (vibrating sample magnetometer).

Kramer doublets. Thus for temperatures $T>T_N$ the magnetic specific heat c_{mag} can be expressed as a Schottky contribution of the $n=3$ Sm^{3+} crystal-field levels (the Δ_i denote the crystal-field level energies in Kelvins, $\Delta_1=0$):

$$c_{mag}=\frac{R_g}{T^2}\left\{\frac{\sum_{i-1}^{n}\Delta_i^2\exp\frac{-\Delta_i}{T}}{\sum_{i=1}^{n}\exp\frac{-\Delta_i}{T}}-\left(\frac{\sum_{i-1}^{n}\Delta_i\exp\frac{-\Delta_i}{T}}{\sum_{i=1}^{n}\exp\frac{-\Delta_i}{T}}\right)^2\right\}. \tag{3}$$

From the analysis we obtain $\gamma=17.0\pm0.3$ mJ/mol K^2, $\Theta_D=220\pm2$ K and $\alpha_D=(1.2\pm0.2)\times10^{-4}$ K^{-1}. The best fit of the Schottky contribution gives the positions of the two excited doublets as $\Delta_2=100\pm5$ K and $\Delta_3=120\pm5$ K, respectively, yielding the high-temperature magnetic entropy $S_{\rm mag}=R_g\ln(6)$, as expected for the Sm^{3+} ion (see Fig. 2).

B. Expansion and magnetization measurements

The magnetic phase diagram of the $SmCu_2$ single crystal has also been investigated by thermal expansion and magnetostriction measurements. Figure 4 shows the field dependence of the thermal expansion along the crystallographic a,b, and c directions. Four phase transitions are observed at 2.0 K, 16.2 K, 16.8 K, and at $T_N=22.7$ K in zero magnetic field and agree well with the results of specific heat (see Fig. 3). Comparing these measurements to available literature data[4,5] we find, that the lowest transition and the intermediate phase above 16 K has not been reported yet. In Ref. 4, however, a transition at 10 K has been reported, which cannot be found in our data.

The thermal expansion determined by capacitance dilatometry agrees well with the results of x-ray powder diffraction above T_N.[5,9] Below T_N strong magnetoelastic effects along the b and c axis appear, which have not been seen in x-ray diffraction. Summing up $\Delta a/a$, $\Delta b/b$, and $\Delta c/c$ leads to a very small volume effect. The thermal expansion measured in a magnetic field shows that there are only very small changes of the transition temperatures in fields along the b direction. The transition temperatures change to 1.8 K, 14.7 K, 15.2 K, and 22.3 K at the maximum-available static field of 15 T. The forced magnetostriction in fields up to 15 T is negligible ($\Delta l/l<3\times10^{-5}$).

Besides the dilatometric experiments, magnetization measurements have been performed in magnetic fields parallel to the crystallographic b direction (see Fig. 5). The magnetization measured at constant fields in the temperature range between 2 K and 30 K yields anomalies at temperatures that are consistent with the values derived from the thermal expansion measurements (e.g., 2.7 K, 15.2 K, 15.6 K, and 21.9 K at 10 T). Below 2.7 K a small increase of the magnetization was detected. However, the two transitions around 15 K cannot be separated because of only small magnetization differences between the phases. The magnetization curves at constant temperatures measured in steady fields up to 14 T show no phase transitions indicating that the transition lines in the magnetic (H,T) phase diagram are nearly vertical in this field range and it is only possible to induce ferromagnetism in higher fields. Therefore, we performed magnetization measurements in pulsed fields at several temperatures. Because of the small value of the magnetic moment in $SmCu_2$ it was necessary to correct the magnetization curve by subtracting the signal without sample from the measured signals for each run. Please note, that both signals are of the same

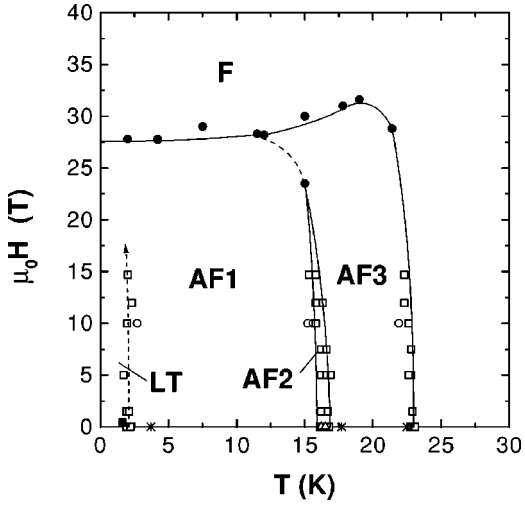

FIG. 6. Magnetic phase diagram of $SmCu_2$ for magnetic field parallel to the crystallographic *b*-direction as deduced from VSM magnetization (open circles), pulsed field magnetization (full circles), magnetostriction (open squares), thermal expansion (full squares), specific heat (stars), and resistivity (triangles) measurements. For the description of the different phases see text.

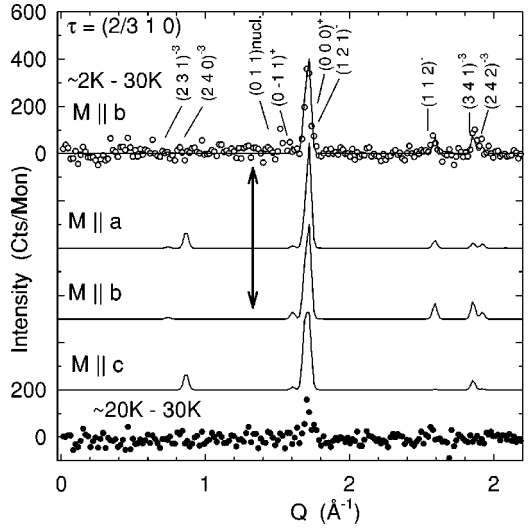

FIG. 7. Difference diffraction pattern at $T=2$ K (top) and $T=20$ K (bottom)—the pattern at 30 K has been subtracted. The line in the top pattern indicates a fit of a squared up structure with a propagation vector of (2/3 1 0). The Sm magnetic moment of $m_b=0.45\ \mu_B$/f.u. is assumed to be aligned parallel to *b* axis. Calculated patterns with the same propagation vector and Sm moment, however, aligned parallel to the *a* and *c* axis are shown for comparison (D1B, $\lambda=0.25$ nm).

order of magnitude. Therefore, the curves shown in Fig. 5 are not as smooth as for measurements in steady fields and the absolute values are correct only within $\pm 20\%$. Nevertheless, the transition fields between 27 T and 29 T can clearly be identified (compare Ref. 10). The transition field value increases with increasing temperature and decreases again near the ordering temperature.

The magnetic saturation moment of $SmCu_2$ along the *b* direction is approximately $0.5\pm 0.1\ \mu_B$/f.u. (see Fig. 5). In addition to crystal-field effects an almost complete compensation of the spin and orbital moment may be the reason for this small value.

The magnetic phase diagram as shown in Fig. 6 is constructed from the available data. At zero field it is characterized by antiferromagnetic order with a low-temperature phase AF1 and, between approximately 16.6 K and the Néel temperature $T_N=23.0$ K, a high temperature phase AF3. Between these two phases an intermediate phase AF2 exists in a narrow temperature region $16.0\ \text{K}<T<16.6$ K (which can be seen most clearly by the two first-order peaks of the specific heat measurement, Fig. 3). Such an intermediate phase was also found in $NdCu_2$ (Ref. 11) and described there as a commensurate phase with an extremely long period and squared up moments. Furthermore, a zero-field phase transition at 2.2 K was found by dilatometric measurements but its origin remains unclear. We propose a low-temperature phase that should be a modification of AF1. In specific heat measurements an anomaly can be seen at a slightly higher temperature of $T=3.7$ K (see inset of Fig. 3). The vibrating-sample magnetometer (VSM) magnetization data also show a low-temperature anomaly characterized by a small increase of the magnetic moment. Measurements using a ^{3}He insert are planned to characterize this low-temperature phase in detail. In magnetic fields the phases are stable up to 28 T, approximately. Above this field value all magnetic moments are oriented parallel to the external field forming the induced ferromagnetic phase F.

The proposed phase diagram resembles the situation of $TbCu_2$ and $DyCu_2$,[10] for which a propagation vector $\tau=(2/3\ 1\ 0)$ was found for AF1. But, in contrast to $SmCu_2$, in $TbCu_2$ and $DyCu_2$ the easy axis of magnetization is the *a* axis. Note also the unusual increase of the transition field AF3—F with temperature, which may be due to a temperature-dependent compensation of the Sm^{3+} spin and orbital moments.[12]

C. Neutron diffraction

Powder neutron diffraction was used in order to determine the magnetic structure of $SmCu_2$. In contradiction to the model expectation[1,3] [predicting $\boldsymbol{\tau}=(2/3\ 0\ 0)$ as outlined in the Introduction] we find a propagation vector of $\boldsymbol{\tau}=(2/3\ 1\ 0)$ at $T=2$ K for the phase AF1. In Fig. 7 the calculated magnetic-intensity pattern is shown in comparison with the experimental data. From these data we infer a magnetic structure that is shown in Fig. 8 in a projection onto the orthorhombic *ab* plane. In the phase AF3 at $T=20$ K the magnetic propagation vector changes to an incommensurate value. Any intensity on the higher-order satellites of the propagation vector $\boldsymbol{\tau}=(2/3\ 1\ 0)$ is within the scatter of the data. In Fig. 9 the magnetic satellites (2/3 1 0), (1/3 1 1), (4/3 1 0), and (2/3 1 2) at 2 K are compared to the corresponding reflections at 20 K. By a careful refinement of the lattice parameters and the magnetic propagation vector at 20 K we find a propagation of $\boldsymbol{\tau}^{\star}=(0.677\pm 0.006,\ 0.989\pm 0.011,\ -0.008\pm 0.013)$. Considering the error involved in these values only a significant shift of *h* can be inferred.

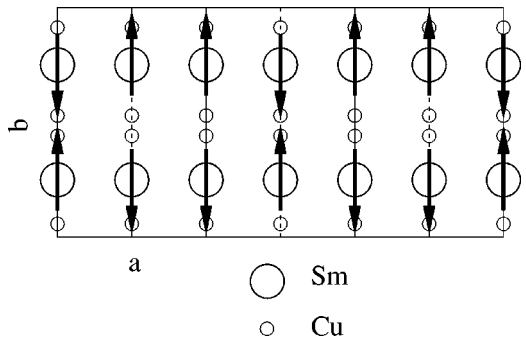

FIG. 8. Magnetic structure of $SmCu_2$ shown in a projection to the ab plane. The magnetic moments are oriented parallel to b. The magnetic unit cell consists of three crystallographic unit cells aligned in a direction.

The antiferromagnetically ordered moment of $m_b = 0.45 \pm 0.07\ \mu_B$/f.u. determined from neutron diffraction in zero magnetic field at $T = 2$ K is in accordance with the saturation moment measured by magnetization.

These results show that the anisotropy of the magnetic exchange interactions in $SmCu_2$ is different in comparison with other RCu_2 compounds. According to the model proposed in Ref. 1 the Fourier transform of the exchange-interaction tensor in RCu_2 compounds can be written as

$$\overline{\overline{\mathcal{J}}}(\mathbf{q}) = \begin{pmatrix} \mathcal{J}^{aa}(\mathbf{q}) & 0 & 0 \\ 0 & \mathcal{J}^{bb}(\mathbf{q}) & 0 \\ 0 & 0 & \mathcal{J}^{cc}(\mathbf{q}) \end{pmatrix} \tag{4}$$

with

$$\mathcal{J}^{aa}(\mathbf{q}) = \mathcal{J}^{cc}(\mathbf{q}). \tag{5}$$

Splitting this interaction tensor into an isotropic and an anisotropic part according to

$$\overline{\overline{\mathcal{J}}}(\mathbf{q}) = \mathcal{J}_{\mathrm{iso}}(\mathbf{q})\,\overline{\overline{1}} + \mathcal{J}_{\mathrm{an}}(\mathbf{q}) \begin{pmatrix} 1 & 0 & 0 \\ 0 & -1 & 0 \\ 0 & 0 & 1 \end{pmatrix}, \tag{6}$$

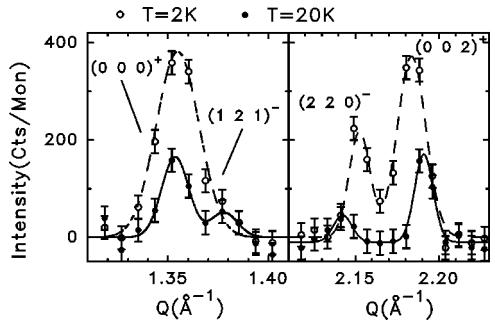

FIG. 9. Magnetic satellites $(0\ 0\ 0)^+$, $(1\ 2\ 1)^-$, $(2\ 2\ 0)^-$, and $(0\ 0\ 2)^+$ at 2 K (open symbols) in comparison with the corresponding reflections at 20 K (full symbols). The lines indicate fits of a Gaussian peaks to the data [with a line width of 0.016 $\mathrm{Å}^{-1}$ (left) and 0.013 $\mathrm{Å}^{-1}$ (right)].

it seems that the sign of anisotropic part $\mathcal{J}_{\mathrm{an}}(\mathbf{q})$ is opposite for $SmCu_2$ in comparison with the other RCu_2 compounds. We believe that such a behavior should have a simple physical reason. However, the microscopic origin of such an anisotropic exchange is still unclear. To show the consistency of our exchange model for $SmCu_2$ [Eq. (6) with $\mathcal{J}_{\mathrm{an}}^{\mathrm{SmCu_2}}(\mathbf{q}) = -\mathcal{J}_{\mathrm{an}}^{\mathrm{other}RCu_2}(\mathbf{q})$] we calculate several physical quantities and compare them to experimental results in the following.

Assuming that the sign of the anisotropy in the exchange tensor is changed for $SmCu_2$ it is possible to estimate some magnetic properties by exchanging the $\mathcal{J}^{aa} = \mathcal{J}^{cc}$ with the $\mathcal{J}^{bb}$ components of the diagonal-exchange tensor, which has been determined for $NdCu_2$.

Following Ref. 1 the Néel temperature can be estimated from

$$k_B T_N = \left(\frac{m_b}{g_J^{\mathrm{Sm}} \mu_B} \right)^2 \mathcal{J}_{\mathrm{Sm}}^{bb}[\boldsymbol{\tau} = (2/3\ 1\ 0)]. \tag{7}$$

Here $g_J^{\mathrm{Sm}} = 2/7$ denotes the Landé factor of the Sm^{3+} ion and $m_b = 0.5\ \mu_B$ the magnetic moment per Sm^{3+} ion as determined from magnetization. Taking for the $\mathcal{J}^{bb}$ component of the exchange in Sm the de Génnes scaled value of the $\mathcal{J}^{aa}$ component in Nd ($\mathcal{J}_{\mathrm{Nd}}^{aa}[\tau = (2/3\,1\,0)] = 79\ \mu\mathrm{eV}, g_J^{Nd} = 8/11$) according to

$$\mathcal{J}_{\mathrm{Sm}}^{bb}[\boldsymbol{\tau} = (2/3\,1\,0)] = \left(\frac{g_J^{Sm} - 1}{g_J^{Nd} - 1} \right)^2 \mathcal{J}_{\mathrm{Nd}}^{aa}[\boldsymbol{\tau} = (2/3\,1\,0)] \tag{8}$$

the expression (7) may be evaluated resulting in a value of 20.0 K for T_N. This is only 13% lower than the experimental value.

By applying the mean-field model developed for $TbCu_2$ and $DyCu_2$ (Ref. 13) to $SmCu_2$ (all these compounds order with the same wave vector) the critical field $H_c^{\mathrm{AF1}\to\mathrm{F}} \| b$ for the transition to the ferromagnetic phase may be calculated using again the $\mathcal{J}^{aa}$ component of the exchange determined in $NdCu_2$.[1]

Using the notation of Ref. 13 in order to number the exchange-interaction constants between the different sublattices the magnetic energies for the antiferromagnetic (AF1) and the ferromagnetic (F) aligned structures (per f.u. and at zero temperature) are given by

$$F_{\mathrm{AF1}} = \frac{m_b^2}{6} \left(\frac{g_J^{\mathrm{Sm}} - 1}{g_J^{\mathrm{Sm}} \mu_B} \right)^2 (2J_2^{bb} - 2J_1^{bb} - 3J_3^{bb} + 3J_4^{bb})$$

$$F_{\mathrm{F}} = -\frac{m_b^2}{2} \left(\frac{g_J^{\mathrm{Sm}} - 1}{g_J^{\mathrm{Sm}} \mu_B} \right)^2 (2J_1^{bb} + 2J_2^{bb} + J_3^{bb} + J_4^{bb}) - \frac{m_b}{k_B} H. \tag{9}$$

The Boltzmann constant k_B in the Zeeman term appears because the exchange parameters J_i and the magnetic energy is calculated in units of K. The critical field $H = H_c^{\mathrm{AF1}\to\mathrm{F}}$ denotes the point at which these two energies are equal ($F_{\mathrm{AF1}} = F_{\mathrm{F}}$) and an expression for $H_c^{\mathrm{AF1}\to\mathrm{F}}$ in terms of the exchange parameters J_i^{bb} may be derived:

$$H_c^{\mathrm{AF1}\rightarrow\mathrm{F}} = -\frac{1}{3}k_B m_b \left(\frac{g_J^{\mathrm{Sm}}-1}{g_J^{\mathrm{Sm}}\mu_B}\right)^2 (2J_1^{bb}+4J_2^{bb}+3J_4^{bb}). \tag{10}$$

Using for J_i^{bb} again the values of J_i^{aa} given for $NdCu_2$ in Ref. 1 (i.e., $J_1^{bb}=2.47$ K, $J_2^{bb}=-2.79$ K, $J_4^{bb}=-3.61$ K) a value of 27.0 T is calculated for $H_c^{\mathrm{AF1}\rightarrow\mathrm{F}}$ that agrees well with the observed transition field of 28 T.

IV. CONCLUSION

The change of the propagation vector in the magnetic phases of $SmCu_2$ resembles closely the behavior of $DyCu_2$ (Ref. 14) (i.e., commensurate at lower temperatures, incommensurate at higher temperatures). However, in contrast to this compound the moment of Sm is aligned parallel to *b*, as found in $NdCu_2$. It should be noted that the Sm^{3+} magnetic moment is rather small due to a compensation of the spin and orbital contributions.

We have shown that the magnetic propagation vector $\boldsymbol{\tau}$, the Néel temperature T_N and the critical field $H_c^{\mathrm{AF1}\rightarrow\mathrm{F}}$ agree with the model calculation, if a sign reversal of the exchange anisotropy in $SmCu_2$ is assumed in comparison to the other RCu_2 compounds. This anisotropy can be described by a symmetric exchange-interaction tensor with vanishing trace. However, the microscopic origin of such an exchange is not clear and we propose further theoretical studies on this subject.

ACKNOWLEDGMENTS

Part of this work was performed within the program of the Sonderforschungsbereich 463 (funded by the Deutsche Forschungsgemeinschaft). Another part of this work was made within the framework of the Research Center for Quantum Materials Physics in the Joint Laboratory for Magnetic Studies, Prague. The authors (P.S. and J.V.) would like to acknowledge the support of the Grant Agency of the Charles University (Grant No. 52/98) and the Grant Agency of the ASCR (Grant No. GAAV D 101 0023).

*Electronic address: rotter@physik.tu-dresden.de

[1] M. Rotter, M. Loewenhaupt, S. Kramp, T. Reif, N.M. Pyka, W. Schmidt, and R.v.d. Kamp, Eur. Phys. J. B **14**, 29 (2000).
[2] M. Loewenhaupt, M. Rotter, and S. Kramp, Physica B **276-278**, 602 (2000).
[3] M. Rotter, M. Loewenhaupt, and S. Kramp, Physica B **276-278**, 598 (2000).
[4] Y. Isikawa, K. Mori, H. Takeda, I. Umehara, K. Sato, Y. Onuki, and T. Komatsubara, J. Magn. Magn. Mater. **76-77**, 161 (1988).
[5] E. Gratz, N. Pillmayr, E. Bauer, H. Müller, B. Barbara, and M. Loewenhaupt, J. Phys.: Condens. Matter **2**, 1485 (1990).
[6] M. Rotter, H. Müller, E. Gratz, M. Doerr, and M. Loewenhaupt, Rev. Sci. Instrum. **69**, 2742 (1998).
[7] H. Krug, M. Doerr, D. Eckert, and H. Eschrig, Physica B **294-295**, 605 (2001).
[8] C.A. Martin, J. Phys.: Condens. Matter **3**, 5967 (1991).
[9] M. Rotter, Ph.D. thesis, Technische Universität Wien, 1994.
[10] M. Loewenhaupt, M. Doerr, L. Jahn, T. Reif, C. Sierks, M. Rotter, and H. Müller, Physica B **246-247**, 472 (1998).
[11] M. Loewenhaupt, T. Reif, P. Svoboda, S. Wagner, M. Waffenschmidt, H.v. Löhneysen, E. Gratz, M. Rotter, B. Lebech, and T. Hauss, Z. Phys. B: Condens. Matter **101**, 499 (1996).
[12] H. Adachi and H. Ino, Nature (London) **401**, 148 (1999).
[13] N. Iwata, Y. Hashimoto, T. Kimura, and T. Shigeoka, J. Magn. Magn. Mater. **81**, 354 (1989).
[14] T. Reif, M. Doerr, M. Loewenhaupt, M. Rotter, P. Svoboda, and S. Welzel, Physica B **276-278**, 600 (2000).